

Thermodynamics of Formation of Porous Polymeric Membrane by Phase Separation Method II. Particle Simulation Approach by Monte Carlo Method and Experimental Observations for the Process of Growth of Primary Particles to Secondary Particles

Kenji KAMIDE,[†] Hideki IJIMA, and Hironobu SHIRATAKI

*Fundamental Research Laboratory of Natural & Synthetic Polymers,
Asahi Chemical Industry Co., Ltd., 11-7 Hacchonawate,
Takatsuki, Osaka 569, Japan*

(Received March 26, 1993)

ABSTRACT: An attempt was made (1) to establish a theory on particle growth during the membrane formation by the phase separation method with an aid of computer simulation technique, and (2) to compare results of the computer simulation with those of actual experiments. In the particle simulation, primary particles consisting of polymer-rich phase are generated at random position in a hypothetical space, and moving velocity v_1 was given to them, assuming Brownian movement in a solution of polymer-lean phase. If a distance between the centers of gravity of two arbitrary chosen particles is less than the summation of their radii, they are considered to have collided, yielding a new larger particle. The simulation reveals that the growth rate of particles is theoretically expected to be larger when the phase separation occurs under the conditions of lower concentration (*i.e.*, lower viscosity) of polymer-lean phase and of smaller two phase volume ratio $R(\equiv V_{(1)}/V_{(2)}$; $V_{(1)}$ and $V_{(2)}$ are the volumes of polymer-lean and -rich phases, respectively). The lower viscosity yields larger velocity and the smaller R gives larger collision frequency. Particle size distribution $N(S)$ and the number-average radius of growing particles \bar{S} were evaluated by dynamic light scattering measurement on systems of polymer solution/coagulating solution, *i.e.*, cellulose cuprammonium solution/acetone-ammonia-water solution and cellulose cuprammonium solution/sodium hydroxide-water solution and it is experimentally confirmed that the primary particles grow by amalgamation and under some conditions, their radii approach an asymptotic value, which is the radius of the secondary particle S_2 .

KEY WORDS Phase Separation / Porous Polymeric Membrane / Primary Particle / Secondary Particle / Particle Growth / Monte Carlo Simulation / Dynamic Light Scattering / Cellulose Cuprammonium Solution /

In the previous paper,¹ we proposed a theory on the nucleation and growth of nuclei to the primary particles in the process of formation of the porous polymeric membranes by the phase separation method, *i.e.*, the solvent-casting method in the case when initial polymer volume fraction v_p^0 is less than polymer volume fraction at a critical solution point v_p^c (steps a—d in Figure 1). The subsequent steps are those, in which the primary particles grow to

the secondary particles (steps d—f in Figure 1). For these steps Kamide and Manabe gave a tentative explanation,² which contains serious mathematical ambiguity and numerous assumptions. The validity of their calculation could not be examined with the actual experiments due to many parameters, being able to be unestimated by the experiments, and the calculations were failed to correlate with the phase diagram of the polymer solution/co-

[†] Present address: Faculty of Education, Kumamoto University, Kurokami 2-40-1, Kumamoto 860, Japan.

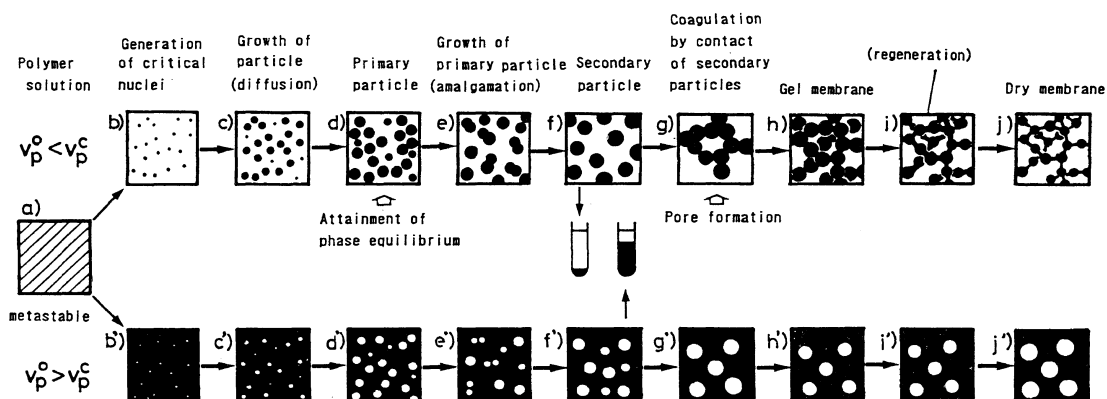


Figure 1. Elementary steps in porous membrane formation by the phase separation method: v_p^0 , initial polymer volume fraction of the solution when the phase separation occurs; v_p^c , polymer volume fraction at a critical solution point.

agulating solution (or non-solvent) system. Smoluchowshi presented a theory on growth of colloidal particles by amalgamation,³ but his theory can't be applied in a system which has particle size distribution.

In this article, we attempted to study the growth of primary particles (steps d–f in Figure 1) by particle simulation approach by Monte Carlo method to give the average size and the particle size distribution as a function of elapsed time, and to compare the results by computer simulation with the actual experiments by dynamic light scattering (DLS) method on systems of polymer solution/coagulating solution, *i.e.*, cellulose cuprammonium solution/acetone–ammonia–water solution and cellulose cuprammonium solution/sodium hydroxide–water solution.

THEORETICAL BACKGROUND

Moving Velocity of the Particles Suspended in Liquid

Moving velocity of particles growing in a phase-separated solution during membrane formation is considered to be estimated by either using the energy equipartition law⁴ or Brownian movement.⁵

Energy Equi-Partition Law. The mean

velocity of primary particle v_1 is given by

$$\frac{1}{2} m_1 v_1^2 = \frac{3}{2} k_B T \quad (1)$$

where m_1 is the mass of the primary particle, k_B , the Boltzmann's constant, T , the Kelvin temperature. We assume the density of the particle ρ to be 1.0×10^3 (kg m^{-3}) and then obtain $m_1 = 4\pi S_1^3 \rho / 3$ (kg). Equation 1 can be rewritten in the form,

$$v_1 = \frac{3}{2} \left(\frac{k_B T}{\pi S_1^3 \rho} \right)^{\frac{1}{2}} \quad (2)$$

where S_1 is a radius of the primary particle.

From eq 2 the velocity of the particle is linearly proportional to $S_1^{-3/2}$. We define Δt as the time needed for a particle with radius of S_1 to move for the distance of $2S_1$. Δt is estimated from S_1 and T through use of the relation

$$\Delta t = \frac{2S_1}{v_1} = \frac{4}{3} \left(\frac{\pi S_1^5 \rho}{k_B T} \right)^{\frac{1}{2}} \quad (3)$$

For a system of cellulose cuprammonium solution/acetone–ammonia–water solution, radius of primary particles S_1 was estimated to be *ca.* 10 nm by using an electron microscope (EM).^{2,6} Accordingly, putting $S_1 = 10$ nm and

Table I. Comparison of Δt

Particle movement	$\Delta t/s$
Energy equi-partition law	1.16×10^{-8}
Brownian movement	2.31×10^{-6}

$T=300$ K, we obtain $\Delta t \sim 1.16 \times 10^{-8}$ s (Table I). It should be noted that, in reality, the particle moves in viscous fluid and therefore, when the energy equi-partition law is employed (eq 1—3), its validity is held only at short distances where the viscosity effects can be neglected.

Brownian Movement. The mean-square displacement of Brownian movement λ^2 of the primary particle at Δt is

$$\lambda^2 = \frac{\Delta t k_B T}{\pi \eta S_1} \quad (4)$$

where η is viscosity of polymer-lean phase surrounding the particle. Then Δt , defined previously, is given by

$$\Delta t = \frac{4\pi \eta S_1^3}{k_B T} \quad (5)$$

If we put $\eta=0.776$ cP for cyclohexane⁷ at θ temperature = 305.1 K⁸ and $S_1=10$ nm and $T=300$ K, we obtain $\Delta t \sim 2.3 \times 10^{-6}$ s (Table I). Equation 4 shows that λ is in linear proportion to $S_1^{-1/2}$, and accordingly, the particle velocity is also proportional to $S_1^{-1/2}$ if particles are assumed to move straight at distance λ . Brownian movement (eq 4 and 5) can not be applied in the case of short-range movement, in which the viscosity effect is neglected. Adequate relation among Δt , v_1 and S_1 differs depending on whether the displacement of $2S_1$ (*i.e.*, in this case, 20 nm) is the distance short enough to neglect the viscosity effect or not. The reasonable answer will be obtained by comparing the simulation with actual experiments.

COMPUTER SIMULATION

The primary particles collide with each other

to yield larger particles which are nominated as growing particles. The growth of the primary particles to the secondary particles with radius of S_2 can be theoretically investigated by using a particle Monte Carlo simulation method in the following manner:

First step: Generate primary particles at random positions in a hypothetical space (cubic body with edge of L'). Assume that all these primary particles have the same radius S_1 of 10 nm. The total number of the primary particles in unit volume N_{PP} (number per m^3) is determined from phase volume ratio R ($\equiv V_{(1)}/V_{(2)}$; $V_{(1)}$ and $V_{(2)}$ are volumes of the polymer-lean and -rich phases, respectively) and S_1 through use of the relation,

$$N_{PP} = \frac{1}{(4/3)\pi S_1^3 (R+1)} \quad (6)$$

Here, we consider only a case when the primary particles consist of polymer-rich phase (*i.e.*, $v_p^0 < v_p^c$). In all calculations, a total number of primary particles generated in a given space $N_{PP}L'^3$ was 2000.

Second step: The movement of these particles starts after completion of generating all the primary particles. This moment is defined as $t=0$. The time of growth of the particles by amalgamation is t . Give a value for velocity of displacement of particles in advance and using this value, determine new positions of all particles randomly after Δt . In other words, the particles are assumed to be engaged in a rapid random motion. Hereafter, Δt , defined as the time needed for a primary particle to move at a distance of its diameter (*i.e.*, 20 nm), is used as unit period of time in calculations.

Third step: Measure the distance between the particles. If a distance between the centers of gravity of two arbitrarily chosen particles (i -th and j -th particles) is less than the summation of the radius of each particle (S_i and S_j), these two particles are considered to have collided, yielding a single larger particle by amalgamation. Here, we assume that volume of the particles is preserved and a radius of this larger

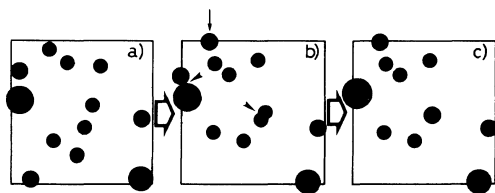


Figure 2. Two-dimensional schematic representation of particle simulation approach: An arrow indicates a particle to which the periodic boundary condition is applied; wedge, particle collision with amalgamation.

particle (S) is calculated to be the cubic root of the summation of the third power of the radii of the two particles before collision as follows:

$$S = (S_i^3 + S_j^3)^{1/3} \quad (7)$$

We consider two types of particle collision in the simulation: One is a case where only the primary particles are assumed to move according to the energy equi-partition law or Brownian movement, and the other is a case where all the particles including the primary particles and larger growing particles are assumed to move based on the energy equi-partition law or Brownian movement. Figure 2 shows two-dimensional schematic representation of the movement and amalgamation of particles in a hypothetical space: The particles, arranged in the manner as Figure 2a, collide with amalgamation (wedges in Figure 2b), resulting in a new arrangement shown in Figure 2c. In the particle simulation approach, the periodic boundary condition, which is applied to a particle with an arrow in Figure 2b, was employed to ascertain the uniformity of a hypothetical space.

After the movement of particles started, steps 2 and 3 are repeated every Δt . If a total number of the particles in a given space was reduced by collision with amalgamation below $1/8$ of $N_{pp}L^3$, the length of the edge of a given space was doubled to continue the calculation. By repeating this treatment, an extended hypothetical space recovers number of particles existing in it up to the number of the primary

particles generated in the originally given space with edge of L , and certainty of calculation can be maintained.

Calculations were carried out using engineering work station model NEWS (manufactured by SONY Corp., Tokyo, Japan).

EXPERIMENTAL

Dynamic Light Scattering Measurement

Cellulose cuprammonium solutions with the weight fraction of cellulose $w_{\text{Cell}} = 0.0025$ and 0.0050 were prepared by diluting an original cellulose cuprammonium solution with ammonium-water solution having the weight fraction of ammonia w_{NH_3} of 0.28 . Compositions of the original cellulose cuprammonium solution are $w_{\text{Cell}} = 0.10$, the weight fraction of copper $w_{\text{Cu}} = 0.0395$, $w_{\text{NH}_3} = 0.0703$, the weight fraction of water $w_{\text{H}_2\text{O}} = 0.7902$.

One part (in volume) of cellulose cuprammonium solution ($w_{\text{Cell}} = 0.0050$) and five parts (in volume) of acetone-ammonia-water solution ($w_{\text{Acetone}} : w_{\text{NH}_3} : w_{\text{H}_2\text{O}} = 0.25 : 0.005 : 0.745$ or $0.30 : 0.005 : 0.695$) or one part (in volume) of cellulose cuprammonium solution ($w_{\text{Cell}} = 0.0025$ or 0.0050) and five parts (in volume) of sodium hydroxide-water solution (the weight fraction of sodium hydroxide $w_{\text{NaOH}} = 0.03$) were mixed in a stopped flow mixer (manufactured by Ohtsuka Electronics Co., Ltd., Hirakata, Japan, model MX-980HD) and the mixture was immediately injected to a cell installed in a dynamic light scattering spectrometer (manufactured by Ohtsuka Electronics Co., Ltd., Hirakata, Japan, model DLS-700) at 293.15 K . The scattered light was measured every 10 s at the direction of a right angle. Measurement was repeated ten times for accumulation of data. The particle size distribution $N(S)$ in number fraction and the number-average radius of growing particles \bar{S} were determined by the histogram⁹ method.

RESULTS AND DISCUSSION

Mobility of Particles

Figure 3 shows the plot of the ratio of \bar{S} obtained in the computer simulation to S_1 , \bar{S}/S_1 against a total number of repetition of a cycle (steps 2 and 3) $N_C (= t/\Delta t)$, under conditions that only the primary particles move based on the energy equi-partition law or Brownian movement. Here, all the primary particles, which are assumed to have generated spontaneously at $t=0$, have the same radius S_1 of 10 nm. Both assumptions of the energy equi-partition law and Brownian movement, yielded the same results. The size of growing particles gradually approaches an asymptotic value of a ratio of the number-average radius of the secondary particles \bar{S}_2 to S_1 , \bar{S}_2/S_1 , which is estimated to be 1.76 for $R=2$, 1.64 for $R=5$, 1.51 for $R=10$, 1.45 for $R=20$ and 1.43 for $R=50$. These are attained within the time of $N_C=10-50$, i.e., $1.16 \times 10^{-7}-5.80 \times 10^{-7}$ s in a case when the energy equi-partition law was assumed and $2.3 \times 10^{-5}-1.2 \times 10^{-4}$ s in a case when Brownian movement was assumed. \bar{S}/S_1 are unrealistically small as compared with the experimental value ($\bar{S}/S_1 > 10$)⁶; suggesting that the conditions of calculation used in Figure 3 (only the primary particles move) can not explain the real phenomenon.

As Kamide and Manabe's tentative theory³ on particle growth was also based on an assumption that only primary particles move, their theory should be regarded as unrealistic from this point of view.

Figure 4 shows the plots of \bar{S}/S_1 against N_C for the two alternative conditions: All particles move according to the energy equi-partition law (broken lines) and all particles move according to Brownian movement (full lines). Here, $R=5$ and 10 were assumed. The values of Δt for both energy equi-partition law and Brownian movement are collected in Table I.

Under the energy equi-partition law, the time necessary for mean particle size to attain size

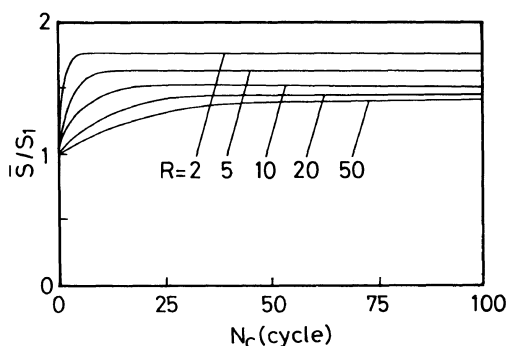


Figure 3. Time-dependence of the ratio of the number-average radius of growing particle \bar{S} to that of primary particle S_1 : The case when only primary particles move. Two-phase volume ratio R is shown in the figure; N_C , a total number of repetition of a cycle (steps 2 and 3) i.e., $t/\Delta t$; $S_1 = 10$ nm; Δt is estimated to be 1.16×10^{-8} s when particles move according to the energy equi-partition law and 2.31×10^{-6} s when particles move according to Brownian movement in viscous media.

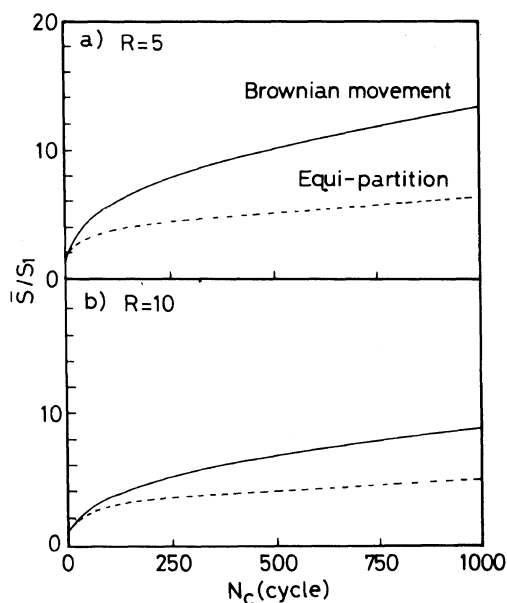


Figure 4. Time-dependence of the ratio of the number-average radius of growing particle \bar{S} to that of primary particle S_1 : N_C , a total number of repetition of a cycle (steps 2 and 3) i.e., $t/\Delta t$; $S_1 = 10$ nm; a), $R=5$; b), $R=10$; broken line, the case when particles of all sizes move according to the energy equi-partition law (eq 1), $\Delta t = 1.16 \times 10^{-8}$ s; full line, the case when particles of all sizes move according to Brownian movement in viscous media (eq 4 and 5), $\Delta t = 2.31 \times 10^{-6}$ s.

of five times as large as the primary particle is estimated to be 5.80×10^{-6} s ($=500\Delta t$) for $R=5$ (a broken line in Figure 4a) and 1.16×10^{-5} s ($=1000\Delta t$) for $R=10$ (a broken line in Figure 4b). Actually, a growing particle grows to approach size of several times as large as that of a primary particle in a few minutes during phase separation for a system of cellulose cuprammonium solution/acetone–ammonia–water solution.⁶ This means that the growth rate seems too large in the case when all particles, *i.e.*, primary particles and other larger growing particles, move according to the energy equi-partition law.

If all particles move according to Brownian movement, the time necessary for mean particle size to attain size of five times as large as the primary particle is estimated to be 1.6×10^{-4} s ($=70\Delta t$) for $R=5$ (a full line in Figure 4a) and 5.8×10^{-4} s ($=250\Delta t$) for $R=10$ (a full line in Figure 4b). The time needed for mean particle size of growing particles to acquire *ca.* eight times of S_1 is *ca.* 6.9×10^{-4} s ($=300\Delta t$) for $R=5$ and *ca.* 2.1×10^{-3} s ($=900\Delta t$) for $R=10$. The time is estimated by assuming that the particles move in pure solvent. In reality the growing particles move in viscous polymer solution and as a result the time needed for particle growth will be much longer if the viscosity of the polymer-lean phase solution η should be taken into consideration. The unit of time Δt employed for calculation is estimated from eq 5, in which η is also a function of the polymer volume fraction of polymer-lean phase $v_{p(1)}$, and the weight-average molecular weight of polymer, dissolved in polymer-lean phase, M_w (eq 9 and 10). The experimental value of \bar{S}/S_1 is larger than 10, suggesting that in order to explain the real phenomenon by the computer experiment, it is much appropriate to employ the condition that all particles move according to Brownian movement than the energy equi-partition law. Hereafter, the particle simulation was carried out, assuming that all particles move according to Brownian movement and the viscosity of polymer-lean

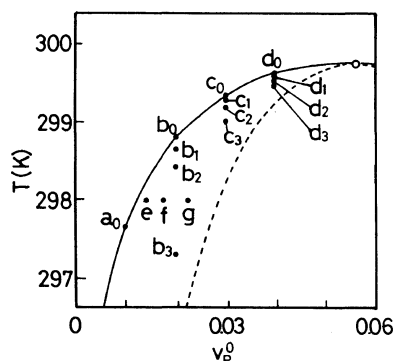


Figure 5. Phase diagram of a system consisting of monodisperse polystyrene ($M = 3 \times 10^5$) and cyclohexane: Full line, coexistence curve; broken line, spinodal curve; open circle, critical solution point; filled circle, point used for calculation of particle growth.

phase η was also taken into consideration.

Effects of the Initial Polymer Concentration v_p^0 and of the Two-Phase Volume Ratio R on the Growth Rate of Particles

We consider a system consisting of monodisperse atactic polystyrene (the molecular weight $M = 3 \times 10^5$) and cyclohexane, whose phase diagram is calculated, based on Kamide and his co-workers' theory^{8,10-12} as shown in Figure 5. Here, we employed the concentration dependence parameters p_1 and p_2 of the polymer–solvent interaction parameter χ in modified Flory-Huggins polymer solution theory, defined in the relation,

$$\chi = \chi_0(1 + p_1 v_p + p_2 v_p^2), \quad (8)$$

to be 0.642 and 0.190,⁸ where χ_0 is a parameter independent of concentration v_p , the polymer volume fraction. In this figure, the co-existence curve (*i.e.*, binodal curve) is represented by a full line and spinodal curve by a broken line and a critical solution point by an open circle. When polymer solutions above the co-existence curve are cooled down to the metastable region, defined as the region between the two curves, the solutions are separated into two phases, *i.e.*, polymer-lean phase and -rich phase, whose volume fraction are $v_{p(1)}$ and $v_{p(2)}$, respectively,

and the growth of particles occurs. The points (small filled circle) in the figure indicate the composition and temperature of the solutions, at which the phase separation employed in the simulation occurs. The phase volume ratio R and $v_{p(1)}$ can be calculated using the co-existence curve and of course, these are not independent variables.

The viscosity of polymer-lean phase η is calculated using the well known empirical relation,¹³

$$\eta = \eta_0(1 + [\eta]v_{p(1)} + [\eta]^2v_{p(1)}^2k_H') \quad (9)$$

where η_0 is the viscosity of the pure solvent, $[\eta]$, the limiting viscosity number ($\text{cm}^3 \text{g}^{-1}$), k_H' , Huggins coefficient. Here, we used the values for the system consisting of atactic polystyrene and cyclohexane at Flory temperature ($\theta = 305.1 \text{ K}$)⁸; $\eta_0 = 0.776 \text{ cP}$ ⁷ and $k_H' = 0.59$.¹⁴ $[\eta]$ is related to the weight-average molecular weight M_w through the Mark-Houwink-Sakurada equation,¹⁵

$$[\eta] = 8.46 \times 10^{-4} M_w^{1/2}. \quad (10)$$

Δt is obtained by substituting η calculated by eq 9 for η in eq 5.

Figure 6a shows the ratio of the number-average radius of growing particles \bar{S} to that of primary particles S_1 , \bar{S}/S_1 as a function of time for a series of solutions, whose locations in the phase diagram are shown as points a_0 , b_0 , c_0 , and d_0 in Figure 5. Note that in these cases all points are located in vicinity to the cloud point curve, assuming that R is 100. Inspection of Figure 6a indicates that the growth rate of the particles is larger for smaller v_p^0 . That is, when R is the same, the particle growth rate is determined by $v_{p(1)}$ and is larger as $v_{p(1)}$ is smaller. This can be reasonably explained in the following manner: The mean square displacement of the particles with the same radius is inversely proportional to η (eq 4), and the mean square displacement is larger, accordingly, the frequency of collision is larger in less viscous media. In addition, the difference in the mean size of particles growing at points

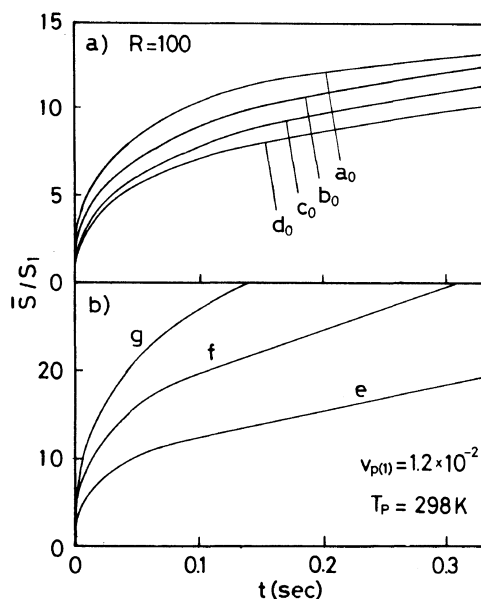


Figure 6. Time-dependence of the ratio of the number-average radius of growing particle \bar{S} to that of primary particle S_1 : a), Effect of v_p^0 at constant R ($=100$); curve a_0 , $v_p^0 = 0.01$, $T = 297.65 \text{ K}$; curve b_0 , $v_p^0 = 0.02$, $T = 298.76 \text{ K}$; curve c_0 , $v_p^0 = 0.03$, $T = 299.53 \text{ K}$; curve d_0 , $v_p^0 = 0.04$, $T = 299.65 \text{ K}$; b), Effect of R at constant $v_{p(1)}$ ($= 1.20 \times 10^{-2}$) and at constant temperature (298 K); curve e , $R = 50$, $v_p^0 = 1.45 \times 10^{-2}$; curve f , $R = 20$, $v_p^0 = 1.80 \times 10^{-2}$; curve g , $R = 10$; $v_p^0 = 2.31 \times 10^{-2}$.

a_0 — d_0 becomes less remarkable, approaching an asymptotic value. The viscosity of the solution influences both the particle growth rate, especially at the initial stage and the time necessary to attain an asymptotic value. The asymptotic value, however, does not depend on η .

Figure 6b shows the particle growth rate of the solutions having various R and constant $v_{p(1)}$ ($= 1.20 \times 10^{-2}$) (points e — g in Figure 5) at constant temperature. The particle grows faster at smaller R when comparison is made at the same $v_{p(1)}$; when R is smaller, the portion of volume occupied by the primary particles is larger, resulting in a rapid increase of the frequency of particle-particle collision.

Effect of Temperature on the Growth Rate of Particles

Figure 7 shows effect of temperature [*i.e.*, depth of phase separation, $\Delta_P (= T_{CP} - T_P$; T_{CP} , temperature at cloud point; T_P , that at phase separation point)] on the number-average radius of growing particles \bar{S} when the solutions having constant v_p^0 , whose locations are shown in the phase diagram (Figure 5) as points d_1 — d_3 for 0.04 (Figure 7a), points c_1 — c_3 for 0.03 (Figure 7b) and points b_1 — b_3 for 0.02 (Figure 7c), are cooled down to different temperatures. Note that in these cases, both R and $v_{p(1)}$ vary concurrently in a very complicated manner, corresponding to a variation of the temperature, as demonstrated as points in Figure 5. Interestingly, the particle growth rate is larger as the phase separation occurs at a point closer to the spinodal curve (*i.e.*, at larger Δ_P ; b_3 , c_3 , and d_3), where the polymer volume fraction of polymer-lean phase $v_{p(1)}$ is lower (and accordingly, its viscosity is lower), resulting in larger velocity of the particles, and simultaneously, R is smaller. Comparison of Figures 7a—7c shows that even at the same R the particles grow much faster from the solutions of lower initial concentration due to lower $v_{p(1)}$ (*i.e.*, lower η).

Summarizing, the growth rate of the particles is theoretically expected to be larger when the phase separation occurs under the conditions of (1) lower polymer volume fraction of polymer-lean phase $v_{p(1)}$ and (2) smaller two-phase volume ratio R . Lower $v_{p(1)}$ yields the larger velocity and smaller R makes for a larger collision frequency. These conditions will be satisfied practically, at least, when a dilute solution is quickly cooled down (or quenched) to a point in the metastable region near to the spinodal curve and kept there for a longer period.

Figures 8a—8c show the particle size distribution, calculated under the conditions shown as points d_1 — d_3 in Figure 5; $v_p^0 = 0.04$; $R = 50$ for Figure 8a, 20 for Figure 8b, and 10 for Figure 8c. The radius of the primary

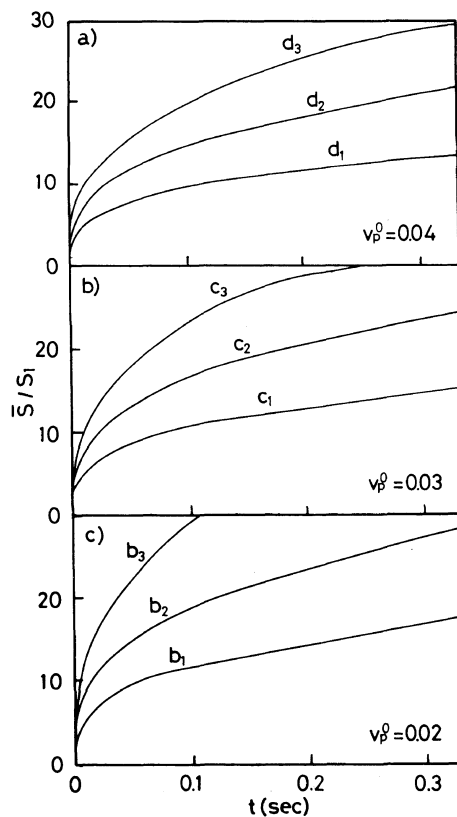


Figure 7. Effect of R and v_p^0 on the relations between the number-average radius of particles and time: a), $v_p^0 = 0.04$; curve d_1 , $T = 299.61$ K, $R = 50$, and $v_{p(1)} = 3.92 \times 10^{-2}$; curve d_2 , $T = 299.58$ K, $R = 20$, and $v_{p(1)} = 3.79 \times 10^{-2}$; curve d_3 , $T = 299.53$ K, $R = 10$, and $v_{p(1)} = 3.62 \times 10^{-2}$; b) $v_p^0 = 0.03$; curve c_1 , $T = 299.26$ K, $R = 50$, and $v_{p(1)} = 2.90 \times 10^{-2}$; curve c_2 , $T = 299.15$ K, $R = 20$, and $v_{p(1)} = 2.62 \times 10^{-2}$; curve c_3 , $T = 299.00$ K, $R = 10$, and $v_{p(1)} = 2.32 \times 10^{-2}$; c), $v_p^0 = 0.02$; curve b_1 , $T = 298.62$ K, $R = 50$, and $v_{p(1)} = 1.83 \times 10^{-2}$; curve b_2 , $T = 298.41$ K, $R = 20$, and $v_{p(1)} = 1.56 \times 10^{-2}$; curve b_3 , $T = 297.29$ K, $R = 10$, and $v_{p(1)} = 7.59 \times 10^{-3}$.

particles S_1 is assumed to be absolutely uniform (*i.e.*, 10 nm). The time of growth t was indicated in the figures. At the very earliest stage, the peak of the size distribution is kept almost at S_1 , but the distribution has a long tail in side of large particle size. As time elapses, the distribution shifts in general to larger S/S_1 region and the width of the distribution became wider with larger R value. After *ca.* 0.2 s, the change of peak position in the particle size

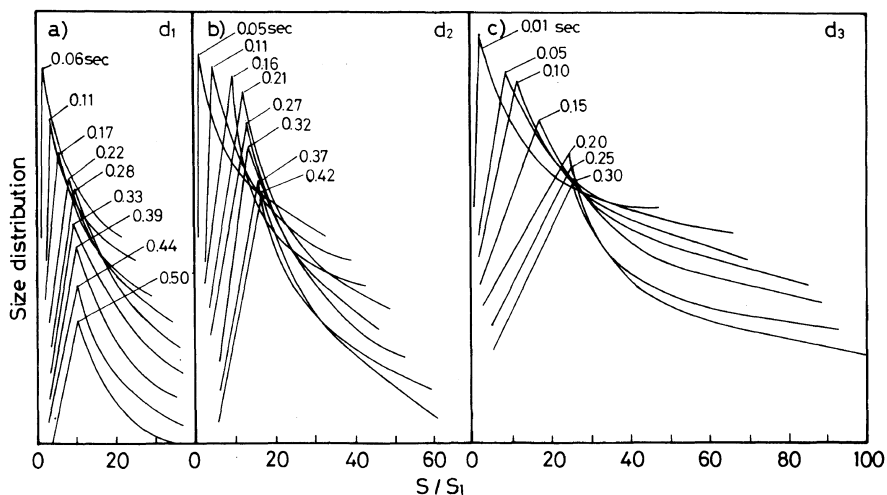


Figure 8. Time-dependence of particle size distribution. Calculations were carried out at points d_1 – d_3 in Figure 5. a), point d_1 ; $T=299.61$ K, $R=50$, and $v_{p(1)}=3.92 \times 10^{-2}$; b), point d_2 , $T=299.58$ K, $R=20$, and $v_{p(1)}=3.79 \times 10^{-2}$; c), point d_3 , $T=299.53$ K, $R=10$, and $v_{p(1)}=3.62 \times 10^{-2}$.

distribution with time became less remarkable. As shown in Figure 7a, the average particle size of growing particles approached its asymptotic value as the time elapsed. Of course, there is neither equilibrium particle size distribution nor equilibrium mean radius of the growing particles and only some approximately steady state, which depends strongly on the time scale of observation, can be realized.

Experimental Observation of Particle Growth

The average size of particles formed in the process of phase separation was experimentally determined by EM observation in a previous paper.⁶ Light scattering measurement provides sound strong scientific evidence, *i.e.*, time dependence of mean particle size and particle size distribution, supporting the “particle growth concept.”

Figure 9 shows particle size distribution $N(S)$ in number fraction, measured by DLS method, as a function of time for a system of cellulose cuprammonium solution ($w_{\text{Cell}}=0.005$)/acetone–ammonia–water solution ($w_{\text{Acetone}}:w_{\text{NH}_3}:w_{\text{H}_2\text{O}}=0.30:0.005:0.695$) at 293.15 K. In this system, $N(S)$ shifts to larger S region with time.

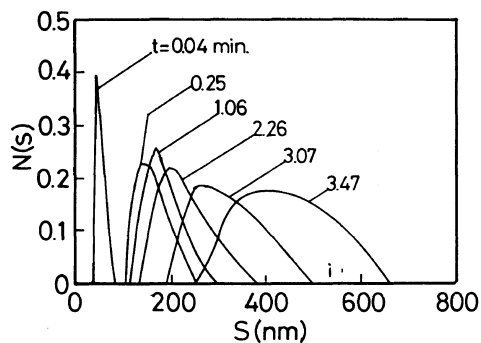


Figure 9. Particle size distribution $N(S)$ in number fraction of a system of cellulose cuprammonium solution/acetone–ammonia–water solution: DLS measurement, one part (in volume) of cellulose cuprammonium solution ($w_{\text{Cell}}=0.005$) and five parts (in volume) of acetone–ammonia–water solution ($w_{\text{Acetone}}:w_{\text{NH}_3}:w_{\text{H}_2\text{O}}=0.30:0.005:0.695$) were mixed at 293.15 K; w_{Cell} in the resulting mixture = 0.00083.

Note that polymer concentration of solutions used for DLS measurement was almost 1/50–1/100 of that of casting solutions actually employed for preparation of membranes from cellulose cuprammonium solutions.

In Figure 10a, $2\bar{S}$ was plotted against time

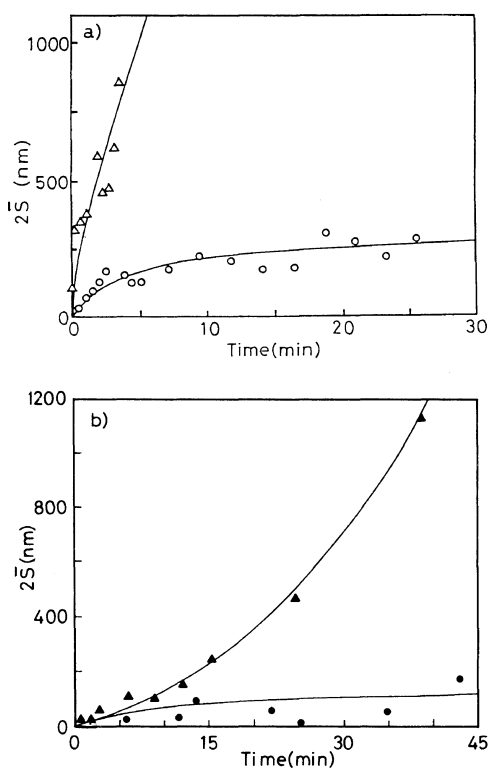


Figure 10. Number-average particle diameter $2\bar{S}$ of four systems of cellulose cuprammonium solution/coagulating solution as functions of time after mixing with the coagulating solution at 293.15 K: a), \circ , mixture of one part (in volume) of cellulose cuprammonium solution ($w_{\text{Cell}} = 0.005$) and five parts (in volume) of acetone–ammonia–water solution ($w_{\text{Acetone}} : w_{\text{NH}_3} : w_{\text{H}_2\text{O}} = 0.25 : 0.005 : 0.745$); \triangle , mixture of one part (in volume) of cellulose cuprammonium solution ($w_{\text{Cell}} = 0.005$) and five parts (in volume) of acetone–ammonia–water solution ($w_{\text{Acetone}} : w_{\text{NH}_3} : w_{\text{H}_2\text{O}} = 0.30 : 0.005 : 0.695$); b), \bullet , mixture of one part (in volume) of cellulose cuprammonium solution ($w_{\text{Cell}} = 0.0025$) and five parts (in volume) of sodium hydroxide–water solution ($w_{\text{NaOH}} = 0.03$); \blacktriangle , mixture of one part (in volume) of cellulose cuprammonium solution ($w_{\text{Cell}} = 0.005$) and five parts (in volume) of sodium hydroxide–water solution ($w_{\text{NaOH}} = 0.03$).

t for two systems consisting of cellulose cuprammonium solution/acetone–ammonia–water solution. $2\bar{S}$ for a system of cellulose cuprammonium solution ($w_{\text{Cell}} = 0.005$)/acetone–ammonia–water solution ($w_{\text{Acetone}} : w_{\text{NH}_3} : w_{\text{H}_2\text{O}} = 0.25 : 0.005 : 0.745$) (open circle) increased rather slowly, approaching to an

asymptotic value (ca. 250 nm) within 10 min, but $2\bar{S}$ for another system of cellulose cuprammonium solution ($w_{\text{Cell}} = 0.005$)/acetone–ammonia–water solution ($w_{\text{Acetone}} : w_{\text{NH}_3} : w_{\text{H}_2\text{O}} = 0.30 : 0.005 : 0.695$) (open triangle) increased very rapidly immediately after mixing. These facts indicate that growth rate of particles change drastically, depending on composition of coagulating solution.

Figure 10b shows time-course change of $2\bar{S}$ estimated for two systems consisting of cellulose cuprammonium solution and sodium hydroxide–water solution ($w_{\text{NaOH}} = 0.03$). Even if composition of coagulating solution is the same, growth rate of particles was different, depending on polymer concentration in the system; $2\bar{S}$ increased slowly when w_{Cell} in a polymer solution before mixing was 0.0025 (closed circle), while $2\bar{S}$ increased much more rapidly with time and continuously, exceeding 1000 nm or more when w_{Cell} in a polymer solution before mixing was 0.005 (closed triangle).

Therefore, it is experimentally confirmed that the primary particles grow by amalgamation and under some conditions their radii approach an asymptotic value, which is the radius of the secondary particle S_2 , and this pattern of growth of particles, directly observed by DLS and EM, is theoretically reasoned. A theoretical treatment used here is reasonable, but not very quantitative to explain the observed phenomenon, because the theory ignores the small, but possible contribution of interfacial properties of particles, such as interfacial free energy, ionic charge and viscosity of particles (*i.e.*, viscosity of polymer-rich phase), whose role can never be underestimated in steps e and f in Figure 1 (*i.e.*, growing particle and secondary particle each).

In order to prepare porous polymeric membranes with desired pore characteristics, it is strongly recommended to choose the conditions under which the secondary particles with the proper radius S_2 are obtained even at pseudo-stable state over a wide range of storage

time. In other words, the extremely slow transition from step d to step f in Figure 1 is an indispensable condition in the solvent-casting process of membrane technology.

CONCLUSIONS

(1) In computer experiments on particle growth during membrane formation by the phase separation method, an assumption that all growing particles move according to Brownian movement is the most appropriate basic tenet for explaining mobility of particles.

(2) The growth rate of the particles is theoretically expected to be larger when the phase separation occurs under the conditions of lower polymer volume fraction of polymer-lean phase $v_{p(1)}$ and smaller two-phase volume ratio R .

(3) DLS measurement showed two patterns of particles growth; gradual growth with approaching an asymptotic value of constant S_2 and rapid and continuous growth without limit, leading to two-phase separation. The computer experiments qualitatively succeeded to simulate the former type of particle growth, giving the secondary particles with approximately constant S_2 .

Acknowledgments. The authors express their sincere gratitude to Mr. Shoichi Ide of BMM Development & Business Promotion Department, Asahi Chemical Industry Co., Ltd. for his technical assistance in DLS measurement.

REFERENCES

1. K. Kamide, H. Iijima, and S. Matsuda, *Polym. J.*, **25**, 1113 (1993).
2. K. Kamide and S. Manabe in "Materials Science of Synthetic Membranes," D. R. Lloyd, Ed., ACS Symposium Series, No. 269, American Chemical Society, Washington, D.C., 1985, p 197.
3. See, for example, J. T. Davies and E. K. Rideal, "Interfacial Phenomena," Academic Press Inc., New York, N.Y., 1961, Chapter 8, p 344.
4. See, for example, W. J. Moore, "Physical Chemistry," 3rd ed, Prentice-Hall, Inc., New York, N.Y., 1960, Chapter 7.
5. See, for example, S. G. Brush, "The Kind of Motion We Call Heat," Book 2, North-Holland Physics Publishing, Amsterdam, The Netherlands, 1986, Chapter 15.
6. K. Kamide and S. Manabe, in "Proceedings of the International Membrane Conference on the 25th Anniversary of Membrane Research in Canada," M. Malaiyandi, O. Kutowy, and F. Talbot, Ed., National Research Council Canada, Ottawa, Canada, 1986, Chapter 2, p 83.
7. "Kagaku-Binran, Kiso-Hen II," 3rd ed, Maruzen, Tokyo, Japan, 1984, p 44.
8. K. Kamide and S. Matsuda, *Polym. J.*, **16**, 825 (1984).
9. E. Gulari, Y. Tsunashima, and B. Chu, *J. Chem. Phys.*, **70**, 3965 (1979).
10. K. Kamide, S. Matsuda, T. Dobashi, and M. Kaneko, *Polym. J.*, **16**, 839 (1984).
11. K. Kamide, S. Matsuda, and M. Saito, *Polym. J.*, **17**, 1013 (1985).
12. S. Matsuda, *Polym. J.*, **18**, 981 (1986).
13. M. L. Huggins, *J. Am. Chem. Soc.*, **64**, 2216 (1942).
14. J. Brandrup and E. H. Immergut, Ed., "Polymer Handbook," 3rd ed, John Wiley & Sons, Inc., New York, N.Y., 1989, Section VII, p 190.
15. H. Inagaki, H. Suzuki, M. Fujii, and T. Matsuo, *J. Phys. Chem.*, **70**, 1718 (1966).